

Gait Event Detection in Tibial Acceleration Profiles: a Structured Learning Approach

Pieter Robberechts^{1*}, Rud Derie^{2*}, Pieter Van den Berghe², Joeri Gerlo², Dirk De Clercq², Veerle Segers², and Jesse Davis¹

¹ Department of Computer Science, KU Leuven
Leuven, Belgium

`first.lastname@cs.kuleuven.be`

² Department of Sport-and Movement Sciences, Ghent University
Ghent, Belgium

`first.lastname@ugent.be`

Abstract. Analysis of runner’s data will often examine gait variables with reference to one or more gait events. Two such representative events are the initial contact and toe off events. These correspond respectively to the moments in time when the foot makes the initial contact with the ground and when the foot leaves the ground again. These variables are traditionally measured with a force plate or motion capture system in a lab setting. However, thanks to recent evolutions in wearable technology, the use of accelerometers has become commonplace for prolonged outdoor measurements. Previous research has developed heuristic methods to identify the initial contact and toe off timings based on minima, maxima and thresholds in the acceleration profiles. A significant flaw of these heuristic-based methods is that they are tailored to very specific acceleration profiles, providing no guidelines on how to handle deviant profiles. Therefore, we frame the problem as a structured prediction task and propose a machine learning approach for determining initial foot contact and toe off events from 3D tibial acceleration profiles. With mean absolute errors of 2 ms and 4 ms for respectively the initial contact and toe-off events, our method significantly outperforms the existing heuristic approaches.

1 Introduction

A gait analysis provides a runner feedback about his running form, enabling him to correct errors and inefficiencies. Typical variables of interest are basic spatio-temporal gait parameters, such as cadence, step length, and ground contact time; as well as more advanced kinematic parameters, such as joint angles, joint velocity and joint accelerations [15]. These variables enable the runner or coach to make more informed decisions regarding the influence of running mechanics upon performance or injury [9]. For example, several studies [2,6] have demonstrated the importance of minimal ground contact time to running performance and

* PR and RD contributed equally to this work.

Willems et al. [22] showed that subjects with altered gait patterns have an increased risk on developing an exercise-related lower-leg injury.

Analysis of gait data will often examine gait variables with reference to one or more gait events. Two such representative events in gait analysis are the initial contact (IC) and toe off (TO) events. These correspond respectively to the moments in time when the foot makes the initial contact with the ground and when the foot leaves the ground again. Determination of these events allows trials to be broken up into gait cycles, consisting of a stance and a swing phase. Many gait variables are defined with reference to either one or both of these gait events. For example, ground contact time (GCT) is defined as the timespan between both events. Also, they function as landmarks that can be used to compare joint angles and forces in between trials, such as knee flexion at IC [10]. Therefore, it is critical that these events are detected accurately and consistently throughout trials.

Whenever the gait data include unambiguous measurement of ground reaction forces (GRF), the IC and TO events can be automatically derived. However, GRF measurements are limited to indoor running facilities and are only possible using expensive equipment. Accelerometer-based systems have been proposed as an ambulatory monitoring solution to deal with the gait analysis [1]. Accelerometers allow continuous, unobtrusive assessment of gait features outside the laboratory environment. As such, they can be used for in-field gait-retraining [23] and gait analysis applications.

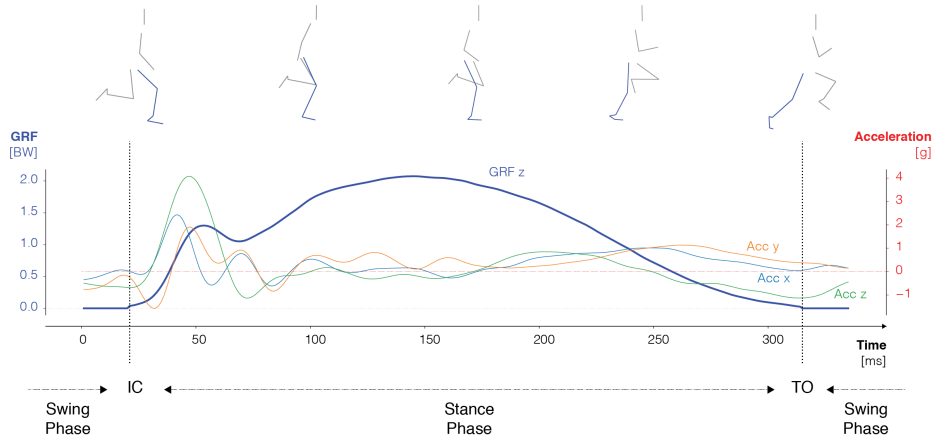


Fig. 1. The gait cycle can be split in a stance phase and a swing phase, separated by the initial contact (IC) and toe-off (TO) events. Ground truth labels are based on the vertical ground reaction force (GRF).

Recently, accelerometers have been extensively used for prolonged outdoor measurements, and various methods referring to sensor locations and detection algorithms have been proposed. In particular, heuristic gait event detection

methods have been developed using accelerometers that are placed on either the foot [1,18,2], lower back [11], or tibia [12,14]. These methods all use a combination of minima, maxima and acceleration thresholds in one or multiple acceleration profiles to detect the IC and TO events. The optimal location of the accelerometers depends on the targeted gait variables, but one interesting location is the tibia. As it is a region that has little soft tissue between the skin and the bone, it is well suited to analyse impact accelerations during running [8]. These impact accelerations are linked to some of the most prevalent injuries within runners, such as tibial stress fractures [21].

A significant flaw of these heuristic-based methods is that they are tailored to very specific acceleration profiles, providing no guidelines on how to handle deviant profiles. For example, Mercer et al. [12] used an accelerometer affixed to the distal aspect of the tibia, identifying IC as a local minima before the peak vertical acceleration and TO as the second local maxima after the peak vertical acceleration. Using a large set of 93 runners, we noticed that the acceleration profiles can widely differ. Often such a clear local minima or second local maxima does not exist.

We propose a machine learning approach for determining IC and TO from 3D tibial acceleration profiles. We define this problem as a structured prediction problem and compare two machine learning approaches: a structured perceptron classifier and a structured deep recurrent neural network (RNN) model. We validated our models by comparing the estimated timings to the timings as determined by the use of a force plate.

2 Methods

This section discusses the used methodology, consisting of data collection, data preprocessing and model construction steps.

2.1 Participants

This study recruited 93 heelstrike runners, both recreational and competitive, from the local running community (55 men and 38 woman; see Table 1 for characteristics). Runners were included if they were free of running-related injuries during the last six months, and ran at least 15 km per week. All subjects signed an informed consent prior to the testing. Approval for the study was obtained from the ethical committee of the Ghent University hospital (2015/0864).

Subjects were instructed to run around our 30 m instrumented running track at different speeds (2.55 m.s⁻¹, 3.20 m.s⁻¹, 5.10 m.s⁻¹ and the subjects preferred running speed). This speed was controlled with timing gates. Runners received feedback if their running speed was not within the ± 0.2 m.s⁻¹ range of the target speed. All subjects wore their own regular training shoes.

Table 1. Characteristics of subjects, expressed as mean \pm standard deviation.

	Men (<i>n</i> = 55)	Women (<i>n</i> = 38)
Age (Yrs)	35.9 \pm 9.2	34.6 \pm 10.8
Body height (m)	1.79 \pm 0.65	1.67 \pm 0.63
Body weight (kg)	76.5 \pm 10.2	60.6 \pm 7.3
Training volume (km/week)	36.4 \pm 16.9	27.9 \pm 11.0

2.2 Equipment

All runners wore on a backpack/tablet system to measure the tibial accelerations. Two tri-axial accelerometers (LIS331, Sparkfun, Colorado, USA; 1000 Hz/axis), were tightly strapped with sport tape on the antero-medial side of both tibiae, eight centimetres above the malleolus medialis [17]. Accelerometers were orientated along the longitudinal axis of the tibia. To improve the rigid coupling between the accelerometers and the tibia the skin around the tibia was pre-stretched with sport tape and secured “as tight as tolerable”, following the recommendations of previous research [17].

Simultaneously, GRF were measured at 1000 Hz by two built-in force platforms (2 m and 1.2 m, AMTI, Watertown, MA). Accelerometer and GRF data were synchronized in time by means of an infrared impulse sent from the Motion Capture system and captured by an infrared sensor at the backpack system.

2.3 Data preprocessing

For each trial which contains at least three steps, we used the vertical component of the GRF to extract the second step in the sequence. For each one of these second steps, we extracted a period ranging from 200 ms before the initial contact to 200 ms after the take-off moment. The other steps were not used: the period before the ground contact of the first step and after the take-off of the last step in each trial is too short to measure the prediction error reliably and the other steps overlap with the period extracted from the second step. Next, we mirrored the data from the left and right leg, such that each of these steps starts with the right foot making ground contact. This preprocessing resulted in a dataset with 1003 examples. One of these examples is shown in Figure 1. Finally, the acceleration signals were filtered using a second-order band-pass filter with cutoff frequencies of 0.8 Hz and 45 Hz. This filter configuration led to the best results during the learning phase.

2.4 Model learning

The problem of predicting the moments of initial contact and take-off can be seen as a structured prediction task.

$$\bar{y}' = \arg \max_{\bar{y} \in \gamma} f(\bar{x}, \bar{y}) \quad (1)$$

Here $\bar{x} = (x_1, \dots, x_T)$ is the input, with each $x_t \in \mathbb{R}^D$ ($1 \leq t \leq T$) a D-dimensional vector that describes the acceleration profile. The goal is to predict the timing of each heel contact event $y_{\text{IC}} \in \{1, \dots, T\}$ and each toe off event $y_{\text{TO}} \in \{1, \dots, T\}$, such that $\bar{y}' = (y_{\text{IC}}, y_{\text{TO}}, \dots)$ is the element of γ that maximizes a scoring function f (i.e., the most likely sequence of IC and TO event timings). For computational feasibility, the scoring functions generally considered are a linear form of a joint feature vector $\Phi(\bar{x}, \bar{y})$:

$$f(\bar{x}, \bar{y}) = w^T \Phi(\bar{x}, \bar{y}). \quad (2)$$

Here w are parameters learned from the data and $\Phi: \chi \times \gamma \rightarrow \mathbb{R}^m$ represents how “compatible” the input sequence \bar{x} is with the output sequence \bar{y} . The length T of each sequence can vary, since strides can have different durations.

In the next sections, we first describe how we construct the feature vectors \bar{x} , followed by a discussion of two possible machine learning approaches to solve this problem.

2.4.1 Feature construction

For each sampled value of each example, we constructed a feature vector from the x, y and z components of the acceleration profiles of both feet. These features include:

Filtered Acc { Left, Right } { x, y, z } The raw values in the acceleration signals at each time step after applying a second order Butterworth bandpass filter at 5-60 Hz.

Filtered Acc { Left, Right } Total The magnitude of the resultant acceleration.

Roll { Left, Right } The roll extracted from the second order Butterworth low-pass filtered acceleration signals at 60 Hz.

Pitch { Left, Right } The pitch extracted from the same low-pass filtered acceleration signals.

Acc { left, Right } { x, y, z, Total } Peak { Min, Max } A moving average filtered labeling of peak values. This marks the neighborhood of a clear peak value for the underlying acceleration signal.

Jerk { Left, Right } { x, y, z } The first derivative of the bandpass filtered acceleration signals.

Jerk { Left, Right } Total The magnitude of the resultant jerk.

Linear trend { slope, standard error } { Left, Right } { x, y, z } The estimated slope of the regression line and standard error of the gradient, using a linear regression fitted on a rolling 20 ms wide frame of the acceleration signal.

This leads to a n by m feature matrix for each example, with $n = 48$ the number of features and m the number of sampled values in the example.

Finally, these features were standardized by removing the mean and scaling to unit variance. This scaling happened independently on each feature and independently for each example.

2.4.2 Structured Perceptron model

We used the structured perceptron algorithm of Collins and Daum [3,5] from the SeqLearn³ package to predict the moments of initial contact and take-off. This is a generalization of the standard perceptron algorithm, which is a simple classification algorithm that makes its predictions based on a linear predictor function combining a set of weights with the feature vector. In a structured learning setting, the core idea is the same. The algorithm makes predictions by choosing the output sequence \bar{y} that maximizes a score given by $w^T \Phi(\bar{x}, \bar{y})$. And if this output sequence is incorrect, it will adjust the weights w toward the correct output sequence \bar{y}' . The only difficulty in this algorithm is the computation of

$$y = \arg \max_{\bar{y} \in \gamma} w^T \Phi(\bar{x}, \bar{y}), \quad (3)$$

which requires searching over all possible output sequences \bar{y} . This is computationally infeasible for long sequences. The key insight is that $\Phi(\bar{x}, \bar{y})$ can be decomposed as $\sum_{i=1}^p \Phi'(\bar{x}, y_i)$. This allows the problem to be solved efficiently using a variant of the Viterbi algorithm.

To determine the optimal set of features and model parameters, we split our dataset into training (83 runners) and test (10 runners) sets. Using cross validation to train the model repeatedly on a randomly selected training set and evaluating it on the test set, we found the following 21 features (as described above) to give the best result: Filtered Acc { Left, Right } { x, y, z }, Filtered Acc { Left, Right } Total, Jerk { Left, Right } { x, y, z }, Jerk { Left, Right } Total, Acc Right x Peak Min, Roll { Left, Right } and Pitch { Left, Right }. Furthermore, we used a learning rate of 0.1, which is the only parameter of this model.

2.4.3 Structured RNN model

The joint feature vector $\Phi(\bar{x}, y_i)$ can be extracted using different techniques. Usually, this is done by handcrafting features as in the structured perceptron model. An interesting alternative for the gait event detection problem is the usage of a Recurrent Neural Network (RNN) model. RNNs are a deep network architecture that can model the behavior of dynamic temporal sequences using an internal state which can be thought of as memory [7]. RNNs provide the ability to predict the current frame based on the previous and/or next frames. As such, the model can learn which long-term patterns in the acceleration profiles are relevant for determining the timings of the gait events.

³ <http://larsmans.github.io/seqlearn/>

We optimize a Recurrent Neural Network (RNN) model and a structured prediction model in an end-to-end fashion. Therefore, we use the structural hinge loss [19]

$$\bar{l}(w, \bar{x}, \bar{y}) = \max_{\bar{y}' \in \gamma} [0, l(\bar{y}, \bar{y}') - w^T \Phi(\bar{x}, \bar{y}) + w^T \Phi(\bar{x}, \bar{y}')] \quad (4)$$

with

$$l(\bar{y}, \bar{y}') = |y_{IC} - y'_{IC}| + |y_{TO} - y'_{TO}|. \quad (5)$$

Since both the loss function and the RNN are differentiable, we can optimize them using stochastic gradient descent (SGD).

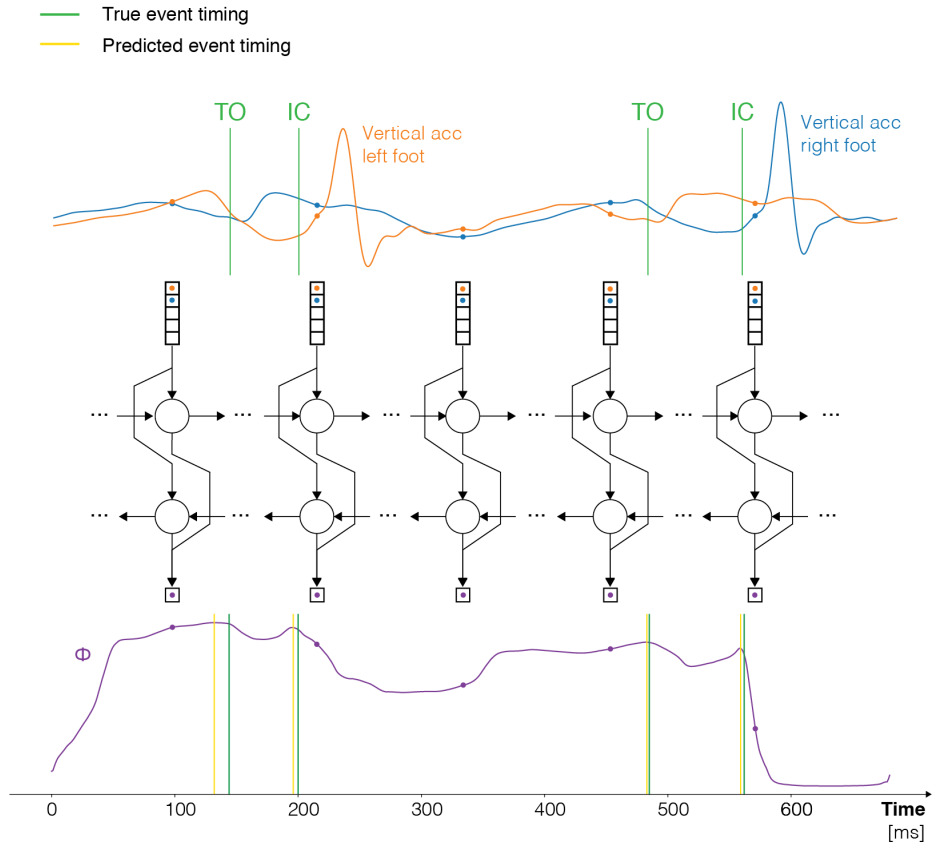


Fig. 2. We use a two-layer bidirectional recurrent neural network with LSTM cells to map the multivariate time series of tibial acceleration profiles (top plot) to the likelihood of an event. Subsequently, a constrained peak detection algorithm is used to determine the most likely timing of IC and TO events. For simplicity, we only plot the vertical acceleration profiles.

Specifically, we use the RNN outputs as feature functions for a structured prediction model (Figure 2). First, an RNN encodes the filtered acceleration signals of an entire stride and outputs a new representation for each of the samples. This new representation corresponds to an approximate likelihood of an event. Then an efficient search is executed over all possible sample values so that the most probable one can be selected. Therefore, we use a constrained peak detection algorithm. This algorithm selects the local maxima that satisfy the following constraints:

- A IC and TO event of the same foot are separated by at least 35 ms and at most 200 ms
- A TO and IC event of opposing feet are separated by at least 160 ms and at most 350 ms

As for the perceptron model, we split our dataset randomly into training (64 runners), validation (10 runners), and test (10 runners) sets to determine the optimal network configuration. Using cross-validation on various parameter and feature combinations, we found the following architecture of the network to give the best results:

- A 20-dimensional time series input consisting of the following features (as described above): Filtered Acc { Left, Right } { x, y, z }, Filtered Acc { Left, Right } Total, Jerk { Left, Right } { x, y, z }, Jerk { Left, Right } Total, Roll { Left, Right } and Pitch { Left, Right }
- Two bidirectional LSTM layers with dropout 0.2 after each recurrent layer
- 50 hidden units

3 Experimental Results

3.1 Baseline methods

Ground truth IC and TO timing were determined using the GRF data. GRF data were first filtered using a Butterworth second-order low-pass filter with a cutoff frequency of 60 Hz. The IC timings were then determined when the vertical GRF exceeded 20 N; the TO timings were determined when the the vertical GRF again fell below 20 N.

Additionally, we used the method defined by Mercer et al. [12] (hereafter referred to as the M-method) to set a baseline for the machine learning models. In this method, the IC and TO timings are defined as the minimum point before positive peak shank vertical acceleration and the minimum acceleration after a second local maxima after positive peak shank vertical acceleration, respectively.

In both methods, GCT was estimated after the IC and TO timings had been obtained as the timespan between both events.

3.2 Evaluation methodology

We performed a leave-one-out cross-validation analysis to estimate the accuracy of our model. The model was iteratively trained on 92 of the 93 test subjects and then the accuracy of the model was tested on the 93th subject. This procedure was repeated 93 times and each time the data of a different subject was left out.

For each step, we calculated both the mean relative error (MRE) and mean absolute error (MAE). Relative errors (RE) were calculated as the arithmetic difference in milliseconds between the predicted event timings (t_{acc}) obtained through the acceleration profiles and reference timings (t_{grf}) obtained through the force-platform method: $RE = t_{acc} - t_{grf}$. A positive value indicated that the detected event occurred after the reference (time lag) and a negative value indicated an early detection (time lead). Absolute errors (AE) were calculated as the absolute value of RE: $AD = |t_{acc} - t_{grf}|$. These are an indicator of the magnitude of the error, regardless of direction.

GCT was subsequently estimated using the obtained gait event estimations. As for the event timings, RE and AE were calculated between the estimated GCT using the accelerometer-based method (GCT_{acc}) and reference (GCT_{grf}): $RD = GCT_{acc} - GCT_{grf}$; $AD = |GCT_{acc} - GCT_{grf}|$. A positive RD corresponds to an overestimate of the GCT, a negative value corresponds to an underestimated GCT.

The number of trials completed by each runner varies substantially. In order to avoid that one runner has an excessively large impact on the accuracy of our models, we compute the global MAE and MRD scores in a two-step procedure. First, for each runner, we compute the average MAE and MRD score over all strides of that runner. Second, the global metrics are then calculated as the average values of these metrics over all runners. This helps prevent the results from being unduly influenced by a single trial or a single runner.

3.3 Results

Our evaluation shows that both machine learning models outperform the heuristic M-method (Table 2). First, we failed to determine the IC and TO events using the M-method in 0.51% and 21.21% of the examples, respectively. These examples did not show clear peaks and valleys in the acceleration profiles. In the cases where events were successfully identified, the M-method detects the IC and TO events considerably earlier ($MRD_{IC} : -9.0 \pm 10.9$; $MRD_{TO} : -32.0 \pm 77.1$). This is in line with the findings in earlier research [13]. In contrast, both the structured perceptron model ($MRD_{IC} : 1.0 \pm 3.8$; $MRD_{TO} : -1.5 \pm 9.7$) and the structured RNN model ($MRD_{IC} : -1.0 \pm 7.8$; $MRD_{TO} : 2.0 \pm 6.0$) have a MRD deviation close to zero. This indicates that the predicted event timings do not consistently lead or lag behind the true event timings. Also, the relatively low standard deviations on the MRD of the ground contact time indicate that both the perceptron ($MRD_{GCT} : -3.0 \pm 10.1$) and RNN model ($MRD_{GCT} : 3.0 \pm 11.0$) can accurately determine a subjects average ground contact time across multiple strides.

Regarding the absolute error, we observe that our RNN model predicts the IC on average within 2.0 ± 7.3 ms of the reference timing. The perceptron model is close with a MAD of 3.0 ± 2.7 ms. This is a substantial improvement compared to the average error of the M-method, which has an MAD of 12.0 ± 7.3 ms. The TO event is considerably harder to predict. Here the RNN model ($\text{MAD}_{\text{TO}} : 4.0 \pm 4.8$) clearly outperforms the other models.

Table 2. MRD and MAD (median \pm standard deviation) between each estimation method and the reference for IC and TO detection (-: time lead; +: time lag) and GCT estimation (-: shorter time; +: longer time)

Variable	Method	Initial Contact	Toe-off	Ground contact time
MRD (ms)	M-method	-9.0 ± 10.9	-32.0 ± 77.1	-24.0 ± 78.5
	Structured perceptron	1.0 ± 3.8	-1.5 ± 9.7	-3.0 ± 10.1
	Structured RNN	-1.0 ± 7.8	2.0 ± 6.0	3.0 ± 11.0
MAD (ms)	M-method	12.0 ± 7.3	43.5 ± 61.5	49.8 ± 58.6
	Structured perceptron	3.0 ± 2.7	12.0 ± 7.4	13.0 ± 7.6
	Structured RNN	2.0 ± 7.3	4.0 ± 4.8	5.5 ± 8.7
Failed predictions (%)	M-method	0.52	21.21	21.73
	Structured perceptron	-	-	0.04
	Structured RNN	-	-	0.11

Bold: minimum MAD for detected IC and TO and estimated ST

Another important feature is the variability of the error, where the risk of an error greater than a given threshold is consistently and significantly lower for our machine learning models compared to the heuristic M-method (Figure 3). Moreover, the RNN model clearly outperforms the perceptron model in terms of error variability. The RNN model is off by at most 10 ms in 80% of the examples, whereas the perceptron model only attains this level of accuracy in 38% of the examples. Yet, despite accurate predictions for most examples, the errors for an individual step can be quite large. For 7% of the examples, the RNN model predicts a ground contact time that deviates at least 50 ms from the reference. Most of them belong to the same four subjects. We manually investigated the acceleration patterns of these cases, but did not discover any clear distinguishing patterns.

The prediction time of the perceptron models are respectively 2 ms and 140 ms.⁴ Compared to an average ground contact time between 200 and 300 ms, this enables real-time gait event detection applications.

⁴ Tested with 2,3 GHz Intel Core i5, 16 GB 2133 MHz LPDDR3 RAM.

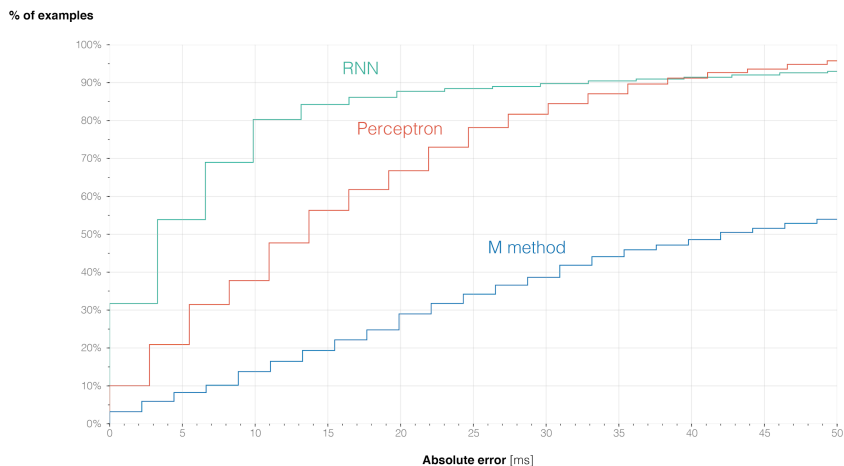


Fig. 3. Comparison of sensitivity (true positive ratio) of three methods as a function of error tolerance (deviation in ms from the true ground contact time, as measured by the gold standard force plate method). Both of our machine learning models outperform the heuristic M method. The RNN model is off by at most 10 ms in 80% of the examples, whereas the perceptron model only attains this level of accuracy in 38% of the examples.

4 Discussion

The purpose of this study was develop a machine learning model for identifying the IC and TO events in tibial acceleration profiles, based on the assumption that both events are associated with typical acceleration features. The IC event can be linked to a quick downward shank movement, coming to an abrupt end when the foot makes ground contact. The TO event, on the other hand, is linked with a quick upward and forward shank movement produced by the knee and hip joint flexion.

We framed this problem as a structured learning problem and evaluated two models: a structured perceptron model with handcrafted features and a structured deep RNN model. The automated methods were validated against a gold standard force plate method and the state of the art heuristic M-method [12].

The M-method detected the IC and TO events consistently earlier and underestimated the GCT. Due to time lag during impact transmission from the feet to the shank, the timing of the manifestation of the acceleration features that distinguish the gait events may differ from the timing of the real gait events. Therefore, heuristic-based methods that use clear patterns in the acceleration profiles to determine the gait event timings result either in a consistent lag or lead in the estimates. Our machine learning models did not suffer from this problem.

Additionally, we observed that the acceleration profiles can differ between subjects and even between different strides of the same subject. The M-method

cannot deal with these variations. It does not define any contingencies for when a peak does not exist, occurs earlier or later than expected, or when multiple peaks are present. Our machine learning algorithms, in contrast, can deal with some limited variability in the acceleration profiles. Although, they are still inaccurate for about 10% of the examples with unique acceleration profiles. Possibly, one might further improve the models by adding data of runners with different patterns. Alternatively, one could train multiple models, one for each gait type. Using principle of transfer learning, one can learn such specific models from a limited dataset [16].

Our method enables accurate real-time gait event detection, which opens up the possibility of gait training with real-time feedback. Accelerometers are light, portable and cheap, such that they can be used outside of the laboratory environment. Recent evidence suggests that gait retraining is effective in reducing impact loading during running [4,20], which has been linked with a series of overuse musculoskeletal injuries [21].

Our research has several limitations. First, it relies on a large training dataset. The collection of this dataset requires a large number of runners, access to a force plate and time. This might impede the adoption of our approach. Secondly, we only evaluated our approach in a controlled setting. All runners ran on the same, flat surface on an indoor track. We are unsure whether our approach generalizes to outdoor running on different terrains.

5 Conclusion

This study showed that a structured RNN learning approach can accurately detect IC and TO events in tibial acceleration profiles, outperforming the currently used heuristic based methods. We compared three approaches to detect gait events: a heuristic-based method, a structured perceptron model with hand-crafted features and a deep learning structured RNN model. We trained and evaluated our models on a large dataset of 93 heel strike runners.

Acknowledgements

This study was funded by the H2020 Interreg EU (Nano4Sports project), the Research Foundation Flanders (FWO.3F0.2015.0048.01) and the KU Leuven Research Fund (C32/17/036).

References

1. Boutaayamou, M., Denoël, V., Brûls, O., Demonceau, M., Maquet, D., Forthomme, B., Croisier, J.L., Schwartz, C., Verly, J.G., Garraux, G.: Algorithm for Temporal Gait Analysis Using Wireless Foot-Mounted Accelerometers. In: Fred, A., Gamboa, H. (eds.) *Biomedical Engineering Systems and Technologies*. pp. 236–254. *Communications in Computer and Information Science*, Springer International Publishing (2017)

2. Chapman, R.F., Laymon, A.S., Wilhite, D.P., Mckenzie, J.M., Tanner, D.A., Stager, J.M.: Ground Contact Time as an Indicator of Metabolic Cost in Elite Distance Runners. *Medicine & Science in Sports & Exercise* **44**(5), 917–925 (May 2012). <https://doi.org/10.1249/MSS.0b013e3182400520>
3. Collins, M.: Discriminative Training Methods for Hidden Markov Models: Theory and Experiments with Perceptron Algorithms. In: *Proceedings of the ACL-02 Conference on Empirical Methods in Natural Language Processing - Volume 10*. pp. 1–8. EMNLP '02, Association for Computational Linguistics, Stroudsburg, PA, USA (2002). <https://doi.org/10.3115/1118693.1118694>
4. Crowell, H.P., Davis, I.S.: Gait retraining to reduce lower extremity loading in runners. *Clinical Biomechanics* **26**(1), 78–83 (Jan 2011). <https://doi.org/10.1016/j.clinbiomech.2010.09.003>
5. Daume, III, H.C.: *Practical Structured Learning Techniques for Natural Language Processing*. Ph.D. thesis, University of Southern California, Los Angeles, CA, USA (2006)
6. Di Michele, R., Merni, F.: The concurrent effects of strike pattern and ground-contact time on running economy. *Journal of Science and Medicine in Sport* **17**(4), 414–418 (Jul 2014). <https://doi.org/10.1016/j.jsams.2013.05.012>
7. Graves, A., Fernandez, S., Gomez, F., Schmidhuber, J.: Connectionist Temporal Classification: Labelling Unsegmented Sequence Data with Recurrent Neural Networks. In: *Proceedings of the 23rd International Conference on Machine Learning*. pp. 369–376. ACM (2006)
8. Hamill, J., Gruber, A.H.: Is changing footstrike pattern beneficial to runners? *Journal of Sport and Health Science* **6**(2), 146–153 (Jun 2017). <https://doi.org/10.1016/j.jshs.2017.02.004>
9. Higginson, B.K.: Methods of Running Gait Analysis. *Current Sports Medicine Reports* **8**(3), 136 (May-June 2009). <https://doi.org/10.1249/JSR.0b013e3181a6187a>
10. Hutson, M., Speed, C.: *Sports Injuries*. OUP Oxford (Mar 2011)
11. Lee, J.B., Mellifont, R.B., Burkett, B.J.: The use of a single inertial sensor to identify stride, step, and stance durations of running gait. *Journal of Science and Medicine in Sport* **13**(2), 270–273 (Mar 2010). <https://doi.org/10.1016/j.jsams.2009.01.005>
12. Mercer, J.A., Bates, B.T., Dufek, J.S., Hreljac, A.: Characteristics of shock attenuation during fatigued running. *Journal of Sports Sciences* **21**(11), 911–919 (Nov 2003). <https://doi.org/10.1080/0264041031000140383>
13. Mo, S., Chow, D.H.K.: Accuracy of three methods in gait event detection during overground running. *Gait & Posture* **59**(Supplement C), 93–98 (Jan 2018). <https://doi.org/10.1016/j.gaitpost.2017.10.009>
14. Norris, M., Kenny, I.C., Anderson, R.: Comparison of accelerometry stride time calculation methods. *Journal of Biomechanics* **49**(13), 3031–3034 (Sep 2016). <https://doi.org/10.1016/j.jbiomech.2016.05.029>
15. Novacheck, T.F.: The biomechanics of running. *Gait & Posture* **7**(1), 77–95 (Jan 1998). [https://doi.org/10.1016/S0966-6362\(97\)00038-6](https://doi.org/10.1016/S0966-6362(97)00038-6)
16. Pan, S.J., Yang, Q.: A Survey on Transfer Learning. *IEEE Transactions on Knowledge and Data Engineering* **22**(10), 1345–1359 (Oct 2010). <https://doi.org/10.1109/TKDE.2009.191>
17. Sheerin, K.R., Reid, D., Besier, T.F.: The measurement of tibial acceleration in runners—A review of the factors that can affect tibial acceleration during running and evidence-based guidelines for its use. *Gait & Posture* **67**, 12–24 (Jan 2019). <https://doi.org/10.1016/j.gaitpost.2018.09.017>

18. Strohrmann, C., Harms, H., Kappeler-Setz, C., Troster, G.: Monitoring Kinematic Changes With Fatigue in Running Using Body-Worn Sensors. *IEEE Transactions on Information Technology in Biomedicine* **16**(5), 983–990 (Sep 2012). <https://doi.org/10.1109/TITB.2012.2201950>
19. Tsochantaridis, I., Joachims, T., Hofmann, T., Altun, Y.: Large Margin Methods for Structured and Interdependent Output Variables. *Journal of Machine Learning Research* **6**(Sep), 1453–1484 (2005)
20. Van den Berghe, P., Lorenzoni, V., Gerlo, J., Breine, B., Derie, R., Six, J., Leman, M., De Clercq, D.: Real-time music-based biofeedback to reduce impact loading during over-ground running. In: 42nd Annual Meeting of the American Society of Biomechanics (ASB). Rochester, MN (2018)
21. Van Der Worp, H., Vrieling, J.W., Bredeweg, S.W.: Do runners who suffer injuries have higher vertical ground reaction forces than those who remain injury-free? A systematic review and meta-analysis. *British Journal of Sports Medicine* **50**(8), 450–457 (Apr 2016). <https://doi.org/10.1136/bjsports-2015-094924>
22. Willems, T., Witvrouw, E., Cock, A.D., Clercq, D.D.: Gait-Related Risk Factors for Exercise-Related Lower-Leg Pain during Shod Running. *Medicine & Science in Sports & Exercise* **39**(2), 330–339 (Feb 2007). <https://doi.org/10.1249/01.mss.0000247001.94470.21>
23. Willy, R.W., Buchenic, L., Rogacki, K., Ackerman, J., Schmidt, A., Willson, J.D.: In-field gait retraining and mobile monitoring to address running biomechanics associated with tibial stress fracture: In-field gait retraining and monitoring. *Scandinavian Journal of Medicine & Science in Sports* **26**(2), 197–205 (Feb 2016). <https://doi.org/10.1111/sms.12413>